Nonwoven as Heat Barrier: Modeling of the Efficiency of Carbtex Fibers

Serge Bourbigot, Sophie Duquesne, Aurore Vannier, Rene Delobel

Laboratoire Procédés d'Elaboration des Revêtements Fonctionnels (PERF), LSPES - UMR/CNRS 8008, Ecole Nationale Supérieure de Chimie de Lille (ENSCL), Avenue Dimitri Mendeleïev - Bât. C7a, BP 90108, 59652 Villeneuve d'Ascq Cedex, France

Received 5 September 2007; accepted 26 November 2007
DOI 10.1002/app.28015
Published online 4 March 2008 in Wiley InterScience (www.interscience.wiley.com).

ABSTRACT: In this work, we examine the use of nonwoven (NW) as heat barrier to protect a metallic substrate. Carbtex fibers consisting in a thermoplastic core inside an oxidized outer shell (polyacrylonitrile or PAN fibers) are selected to make the NW. Measuring temperature profiles in a heat radiator test; it is revealed that Carbtex NW is an efficient heat barrier. A macroscopic model is then developed to simulate heat transfer in NW (considered as a porous medium) used as a protective heat barrier on aluminum plate. The model is validated comparing experimental results obtained by the heat radiator test and predicted values. The efficiency of NW layer is simulated varying different parameters characteristic of the NW (porosity and heat conductivity) and of the design (thickness of the layer). It is revealed to get good efficiency of the NW heat barrier that heat conductivity of the fibers is crucial to get superior performance as well as high porosity (higher than 0.5) associated with a reasonable thickness of NW (5–7 mm). © 2008 Wiley Periodicals, Inc. J Appl Polym Sci 108: 3245–3255, 2008

Key words: nonwoven; heat transfer; modeling; Carbtex; numerical simulation; heat barrier

INTRODUCTION

Nonwoven (NW) is a generic term used to describe a fabric that is produced differently from a fabric made by weaving or, more broadly, a fabric that is different from traditional woven or knitted fabrics.[1] It is an important textile product of tomorrow. Uniquely and variously designed, NW can have the structure and properties of cloth, which is responsible for their increasingly wide use in different branches of the economy and unprecedented growth in comparison to traditional textile products. NW is a versatile material and has the function of moisture impermeability, absorption of liquids, drainage, combustion inhibitors, filtration, and multifunctional barriers.[2] They can be used as products of commodity (e.g., disposables) as well as high performance materials (e.g., hot gas filter or fire blockers). It is our purpose in this article to use NW as potential flexible heat barrier for materials.[3–6]

Like all fabrics, NWs are planar structures that are relatively flat, flexible, and porous. Unlike traditional fabrics that are made by mechanically interlacing (weaving) or interlooping (knitting) yarns composed of fibers or filaments, NW fabrics are made by mechanically, chemically, or thermally interlocking layers or networks of fibers, filaments, or yarns; interlocking fibers or filaments concurrent with their extrusion; perforating films; or forming porous films concurrent with their extrusion.[1] The porosity of NW provides for the materials insulative properties of interest since air is embedded in the structure.[7] NW due to their bulk internal voids, are generally good insulators and are widely used for insulation purposes. In general, heat transfer in NW involves combined modes of heat transfer: radiation within fibers and between fibers, conduction through fibers, and natural convection in spaces. Fibrous materials are commonly used as thermal insulation in many engineering systems due to their effect in reducing the radiation heat transfer.[8–10]

NW is a porous medium; it means it is a material consisting of solid matrix (the fibers) with an interconnected void. The interconnectedness of the void (the pores) allows the flow of one or more fluids through the material. In our situation there is a single phase flow constituted by the air. In NW, the distribution of pores with respect to shape and size is irregular. On the pore scale (the microscopic scale) the flow quantities (velocity, pressure . . .) will be also irregular. But in typical experiments the quantities of interest are measured over areas that cross many pores, and such space-averaged (macroscopic)

Correspondence to: S. Bourbigot (serge.bourbigot@ensc-lille.fr).

Contract grant sponsor: FP-6 European project FLEXIFUNBAR (''Multifunctional barrier for flexible structure'').

quantities change in a regular manner with respect to space and time, and hence are amenable to theoretical treatment. It will be our approach in the following.

Our purpose is to protect a substrate from heat and/or fire using NW materials. Potential applications are the protection of plastic parts from heat source in an engine compartment of automobiles (engine compartments are required to be compact and light) and the making of heat and fire barrier in trains to avoid fire spread. So, those types of applications require NW made with high performance fibers. Carbtex fiber consists of a thermoplastic core inside an oxidized outer shell (polyacrylonitrile or PAN fibers) and Carbtex NW of different densities should be available on the market. The advantage of Carbtex or PAN is that it exhibits superior thermal stability combined with low flammability.[11] The applications of Carbtex include: protective clothing, aircraft fire-block and insulation, and wide range of acoustical and thermal shields for the automotive industry. It is then a material of choice for our applications.

This article is organized in three parts. The first part will present our experimental set-up with the associated protocol to evaluate the efficiency of a heat barrier. A mathematical model will be proposed to simulate heat transfer in NWs used to protect a solid substrate in the second part. In the third part, equations will be solved by finite element method using the commercial package Comsol Multiphysics. Simulations will be then compared with experimental results and discussed.

EXPERIMENTAL CONFIGURATION AND PROCEDURE

Materials

NW made with Carbtex fibers was used as heat barrier for protecting an aluminum plate. Aluminum plate exhibiting a surface of 10×10 cm^2 and a thickness of 3 mm was employed as substrate. Carbtex NW is a needle punched NW exhibiting a density of 600 g/m^2. The use of a high density NW avoids the shrinkage of the material upon heating and so, it permits to consider NW as a solid without deformation during the test. Scanning electron microscopy (SEM) picture reveals that NW is constituted by crossed fibers embedding interconnected voids as postulated in the introduction (Fig. 1). The porosity φ is usually defined as the fraction of the total volume of the medium that is occupied by void space.[7] Thus $1 - \varphi$ is the fraction that is occupied by solid (here the fibers). In defining φ in this way, we have assumed that all the void space is connected. According to the structure of NW (Fig. 1), this assumption is reasonable. To determine the porosity using SEM, the images have been converted into binary image where the features are converted into a number of connected pixels within a specified (grayness of 0–255) threshold range. Pixels are connected if they are horizontal, vertical, or diagonal. Image processing was done using the plug-in Fovea Pro of Photoshop. This method has some limitation because it is highly dependent and limited by the image quality as well as by the subjectivity due to the grayness threshold selection and adjustment. Our SEM images were of good quality and we estimate to $\pm 2\%$ inherent error due to grayness threshold selection. They are also two dimensional in nature which can induce other errors. Making image analysis on 10 representative pictures and using different magnifications, we have estimated the porosity φ equaling 0.75 ± 0.02.

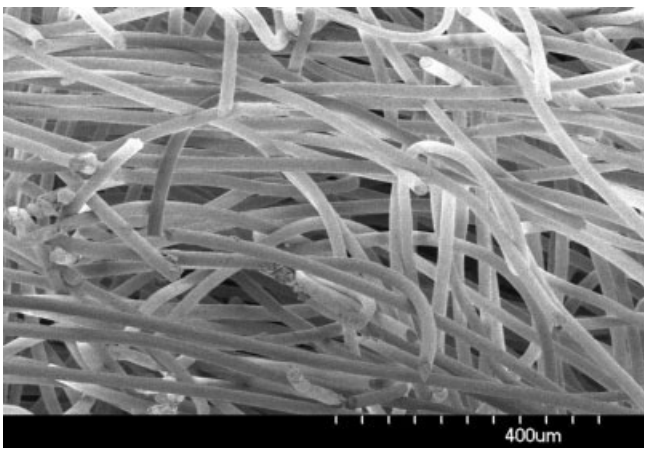

Figure 1 SEM picture of Carbtex NW.

Heat radiator test

In our laboratory, we have recently developed a small scale test permitting to measure the efficiency of a heat barrier. The upper side of an assembly (protective material + substrate) undergoes an external heat flux and the temperature as a function of time is recorded on the backside of the substrate (material to be protected).[12] Using this experimental set-up, we have shown good correlation with large scale test (industrial furnace test) in the case of intumescent paint protecting steel (intumescence means a dynamic expansion of a carbonaceous structure upon heating[13]).

In our test, the heat source is a heat radiator. Aluminum plates (used as substrate to be heat protected in this work) are painted by a black coating, provided by Medtherm Corp. (Huntsville, Al), resistant to 800°C and having a constant emissivity of 0.92. It is applied on the nonheated side of the aluminum

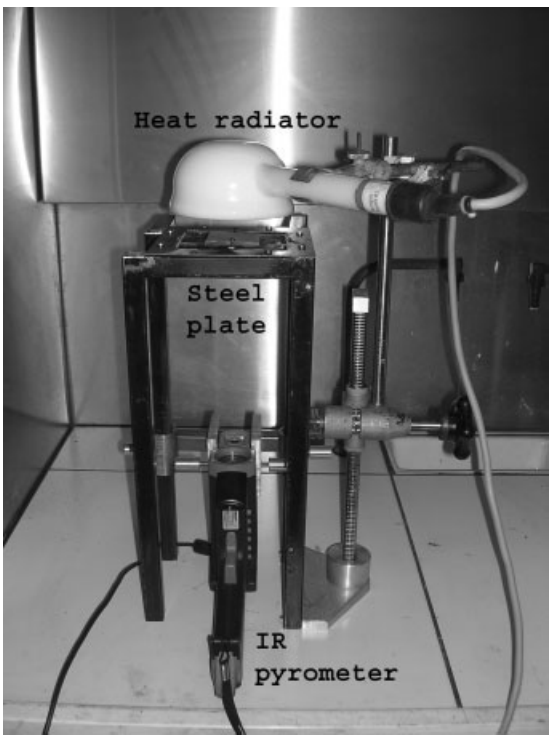

Figure 2 Small scale test to measure the efficiency of a heat barrier.

plates. The constant emissivity of the backside of the plate allows accurate measurement of the surface temperature of the plate using an infrared pyrometer. The infrared pyrometer is at a constant distance from the aluminum plate and the beam is pointed on the center of the plate. It detects the temperature on the nonheated face of the steel plate and records the time/temperature curve on a computer (Fig. 2). NW as heat barrier is put on the aluminum plate (Carbtex NW of 7 mm thick). This small scale test is very stable and repeatable (error on temperature measurement is less than 2%). The whole system is placed into a metallic box to avoid additional convective and chimneys effects due to the surrounding.

MATHEMATICAL FORMULATION

Governing equations

Our purpose is to write the equation that expresses the first law of thermodynamics in porous medium (NW).[14] According to our image analysis made on SEM pictures, a reasonable assumption is to consider the medium (NW) as isotropic. We then assume that viscous dissipation and the work done by pressure changes are negligible. It is also reasonable to assume that there is a local thermal equilibrium so that $T_s = T_f = T$, where T_s and T_f are the temperatures of the solid and fluid phases, respectively. Our last assumption is that heat conduction takes place in parallel so that there is no net heat transfer from one phase to the other. Using those assumptions, we have [eq. (1)]

$$(\rho c_p)_m \frac{\partial T}{\partial t} + (\rho c_p)_f \mathbf{u} \cdot \nabla T = \nabla \cdot (k_m \nabla T) + S_r \quad (1)$$

where the subscript m means the medium (here air + PAN fibers), $(\rho c_p)_m = (1 - \varphi)(\rho c_p)_s + \varphi(\rho c_p)_f$ and k_m is the thermal conductivity of the medium. Here the subscripts s and f refer to the solid and fluid (air) phases, respectively, c_p is the heat capacity, ρ the density, k is the thermal conductivity, and S_r is the radiative source term. Note that in this equation, no term for the heat production per unit volume is added because PAN fibers are not degraded during the test and no exo–endothermal phenomena were detected (or it was negligible). The additional term; $(\rho c_p)_f \mathbf{u} \cdot \nabla T_f$ ($\mathbf{u}$ is the velocity field); is due to the convection of the air into the medium (convective term due to the seepage velocity). It is to be noticed that convection is very often neglected when modeling heat transfer in fibrous materials[4–6] Here, we want to investigate whether the convection may be ignored or should be included in the models as sometimes suggested in the literature.[15]

Fricke and Stark[16] showed that in fibrous insulations the combined solid and gaseous thermal conductivity is underestimated if the thermal conductivity of the gas and thermal conductivity of the solid fibers are superimposed linearly. They developed a basic model where k_m can be calculated for specimens with any fiber orientation by use of a parameter Z, which represents the fraction of all fibers oriented perpendicularly to the macroscopic heat flow. It is also assumed that (i) the fibrous insulation can be approximated as a homogeneous medium of thermal conductivity k_m, (ii) the interactions between fibers influencing k_m can be averaged over a unit volume, and (iii) any individual fiber is assumed to be a spheroid whose major axis is very large compared with the minor axis. All those assumptions are acceptable applied to Carbtex NW. According to this model, thermal conductivity is given by [eq. (2)]

$$k_m = k_s \left[1 + \frac{C_r - 1}{1 + V_r(1 + Z\,(C_r - 1)/(C_r + 1))} \right] \quad (2)$$

where V_r is the ratio of the volume of fiber and gas (here air), Z is the part of all fibers that are oriented perpendicular to the microscopic heat flow (here for randomly oriented fibers $Z = 0.66$), and C_r is the ratio of thermal conductivity of gas (air) to thermal conductivity of solid fibers.

Previous studies[8,17] about heat transfer in fibrous material have shown that radiative heat transfer might constitute a non-negligible part of the total

heat. The radiative source term S_r included in the eq. (1) takes into account this phenomenon. S_r can be expressed as a function of the total radiative heat flux q_r by [eq. (3)]

$$S_r = -\nabla \cdot q_r \tag{3}$$

where $q_r = \int_0^\infty \int_{4\pi} I_\lambda d\Omega d\lambda$ and Ω is the solid angle, I_λ is the radiative intensity, and λ the wavelength. Lee and Cunnington[6] modeled the radiative thermal conductivity of an optically thick medium by a diffusion approximation in which the spectral extinction properties are calculated by a rigorous treatment of the fiber medium scattering phase function and the composition of the fiber material. They modified the classical diffusion model to take into account the effect of scattering by fibers. They demonstrated that the heat transfer by radiation and conduction are additive for optically thick fibrous material (Carbtex NW may be considered as optically thick material). Considering this and introducing k_r, the radiative thermal conductivity, eq. (1) can be rewritten by [eq. (4)]

$$(\rho c_p)_m \frac{\partial T}{\partial t} + (\rho c_p)_f \mathbf{u} \cdot \nabla T = \nabla \cdot ((k_m + k_r)\nabla T) \tag{4}$$

Note that k_r is an experimental parameter which must be measured to be included in the modeling. Measurement methods and results will be discussed in the next section.

The velocity field of the fluid $\mathbf{u}$ is calculated coupling Navier-Stokes equation [eq. (5)] and the equation of continuity for a compressible flow (air) [eq. (6)] with the heat diffusion equation assuming that (i) air confined in NW leads to small density variations due to temperature differences, and that (ii) there are low velocities and no compression/expansion of the fluid (air) resulting in substantial internal work or heat effects. We also assume that the volume force is zero because gravitational forces due to changes in density most likely have very little impact on the model.

$$\rho \frac{\partial \mathbf{u}}{\partial t} + \rho(\mathbf{u} \cdot \nabla)\mathbf{u} = \nabla \cdot \Big[-pI + \eta(\nabla \mathbf{u} + (\nabla \mathbf{u})^T) - (2\eta/3 - \kappa)(\nabla \cdot \mathbf{u})\mathbf{I}\Big] \tag{5}$$

$$\frac{\partial \rho}{\partial t} + \nabla \cdot (\rho \mathbf{u}) = 0 \tag{6}$$

where p is the pressure, $\mathbf{I}$ the identity matrix, η is the dynamic viscosity and κ is the dilatational viscosity.

Note that the equations written above are only valid in NW. Since NW is put on aluminum plate, the classical heat conduction equation[14] should be applied in the solid [eq. (7)]

$$(\rho c_p)_{\text{alu}} \frac{\partial T}{\partial t} = \nabla \cdot (k_{\text{alu}} \nabla T) \tag{7}$$

where the subscript alu refers to aluminum.

Boundaries

Heat radiator heats up the surface of Carbtex NW. It can be assimilated as a hot plate (surface temperature of about 1000 K) exchanging heat with NW via radiative heat transfer). It permits to calculate the net radiative heat flux, q, into NW. Our problem is a typical case of surface-to-surface radiation. In the general case, the irradiation at a given point on the surface derives from the geometry and local temperatures of the surrounding boundaries as well as the temperature of the ambient surroundings. Consider a point on a surface as in Figure 3, point $\bar{x}$ ''sees'' other points on other surfaces as well as the ambient surroundings. Assume that points on the other surfaces have a local radiosity, J', while the ambient surroundings have a constant temperature, T_{amb}.

It can be demonstrated that the resulting expression for the irradiation, G, at $\bar{x}$ is [eq. (8)]

$$G = \int_{s'} \frac{(-\bar{n}' \cdot \bar{r})(\bar{n} \cdot \bar{r})}{\pi |\bar{r}|^4} J' dS + F_{\text{amb}} \sigma T_{\text{amb}}^4 \tag{8}$$

where J' is the radiosity, σ is the Stefan-Boltzmann constant ($\sigma = 5.67\ 10^{-8}$ W/(m^2 K^4)), the integral over S' is a surface integral, and F_{amb} is the view factor for the ambient surroundings [eq. (9)][14]

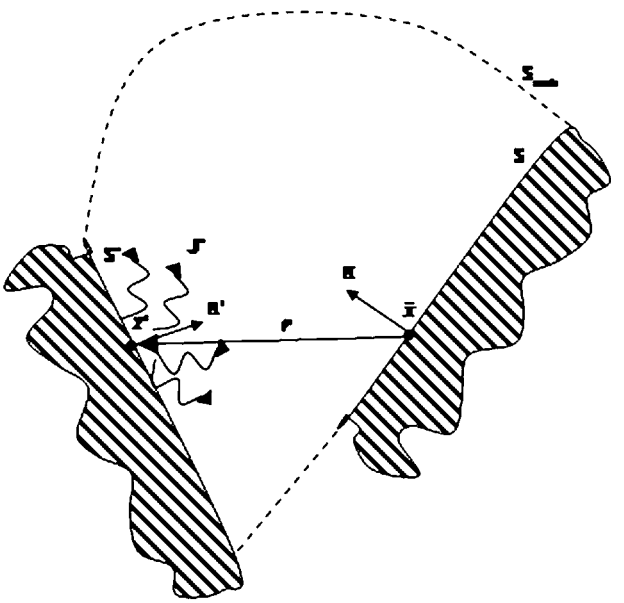

Figure 3 Surface to surface radiation between two surfaces.

$$F_{\text{amb}} = 1 - \int_{s'} \frac{(-\overline{n}'.\overline{r})(\overline{n}.\overline{r})}{\pi|\overline{r}|^4} dS \quad (9)$$

From this above calculation, we can write the boundary conditions for the eqs. (1) and (7). According to the configuration of the test, Dirichlet condition is applied. On the upper surface (NW surface undergoing the heat flux from the heat radiator), it can be written [eq. (10)]

$$-n(-k\nabla T + \rho c_p u T) = h\,(T_{\text{inf}} - T) + \varepsilon\,(G - \sigma T^4) \quad (10)$$

where h is the convective heat transfer coefficient (the calculation of h as a function of temperature will be presented in the next section) and T_{inf} is a reference temperature taking the temperature of the surrounding fluid.

On the sides of NW, the boundary conditions are [eq. (11)]

$$-n\,(-k\nabla T + \rho c_p u T) = h\,(T_{\text{inf}} - T) + \varepsilon\sigma\,(T_{\text{amb}}^4 - T^4) \quad (11)$$

On the backside and on the sides of the aluminum plate, the boundary conditions are written as above without the convective term [eq. (12)]

$$-n\,(-k\nabla T) = h\,(T_{\text{inf}} - T) + \varepsilon\sigma\,(T_{\text{amb}}^4 - T^4) \quad (12)$$

Equations (5) and (6) are only applied in NW and also required boundary conditions. At the interface NW – aluminum plate, no slip condition is used [eq. (13)]

$$\mathbf{u} = 0 \quad (13)$$

On the upper side of the NW and on the four sides of the NW, constant pressure condition is used [eq. (14)]

$$\left[-p\mathbf{I} + \eta(\nabla\mathbf{u} + (\nabla\mathbf{u})^T) - (2\eta/3 - \kappa)(\nabla\cdot\mathbf{u})\mathbf{I}\right]\mathrm{n} = -p_0\mathrm{n} \quad (14)$$

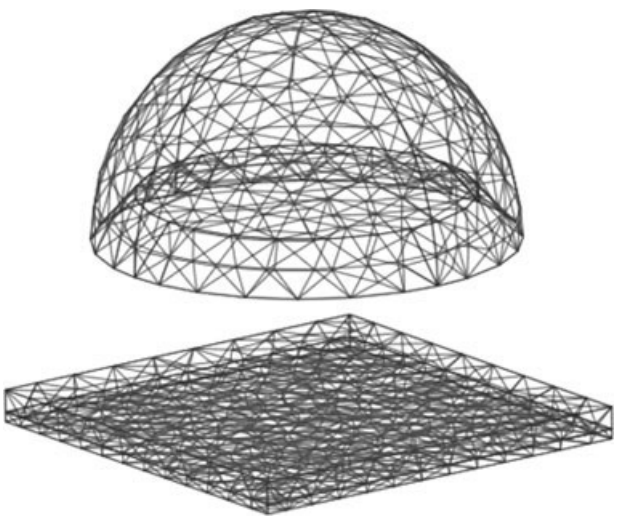

Figure 4 Meshes on heat radiator test.

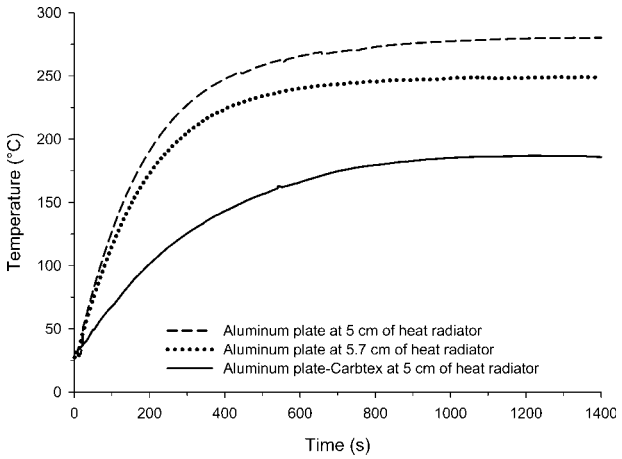

Figure 5 Temperatures as a function of time measured on the backside of aluminum plate with and without Carbtex.

Meshes

After drawing our set-up in 3 dimensions, a 3D mesh is generated as an unstructured mesh containing 5084 tetrahedral elements (Fig. 4). It corresponds to 16,800 degrees of freedom (DOF). Different size domains were also evaluated containing 260 (DOF = 1187), 1323 (DOF = 5238) and 7945 (DOF = 24,322) elements and it was found that the best compromise between the computing time and the accuracy was the grid containing 5084 elements. In the conditions discussed in the next section, the smallest size domain requires 72 s to be solved while that containing 7945 elements requires 1170 s.

RESULTS AND DISCUSSION

NW as heat barrier

The first step of this work is to examine the efficiency of Carbtex NW as heat barrier on a substrate. Temperature as a function of time is measured on the backside of the substrate (aluminum) with and without Carbtex using our heat radiator test (Fig. 5). Note that the aluminum plate alone was evaluated at two distances of the hot plate of the heat radiator. The purpose is to measure the effect of Carbtex if the whole assembly is at the same distance as the aluminum plate alone or if Carbtex is put onto the aluminum plate remaining at a constant distance from the heat source. As expected, temperature on the backside of the aluminum plate at the shortest distance increases more rapidly and reaches a higher temperature than that located further (275°C vs. 240°C at 1400 s). The interesting feature is that Carb-

tex NW provides a real heat protection of the aluminum plate. The heating rate of the assembly aluminum + Carbtex is strongly decreased compared with the aluminum plates alone (0.35°C/s versus 0.7°C/s) and the temperature reaches only 175°C compared to 240°C (or 275°C) at 1400 s. It demonstrates that NW Carbtex can be used as heat barrier.

Radiative thermal conductivity

In our application, the optical thickness of the Carbtex thermal insulation is large. For an optically thick medium, radiation travels only a short distance before being scattered or absorbed. The energy transfer depends only on the conditions in the intermediate vicinity of the position being considered. It is the so-called diffusion approximation and the radiative heat flux can be expressed as [eq. (15)][18]

$$q_r = -\frac{16\sigma T^3}{3\sigma_{e,R}}\frac{\partial T}{\partial x} = -k_r\frac{\partial T}{\partial x} \tag{15}$$

where $\sigma_{e,R}$ is the Rosseland mean extinction coefficient. In real applications and for optically thick material, the value of k_r is modified taking into account the effective index of refraction, n (note that n should be understood as the index of the homogeneous equivalent medium and an acceptable value is 1 for highly porous media as NW), and is approximated by the Rosseland equation as [eq. (16)][18]

$$k_r = \frac{16n^2\sigma T^3}{3\sigma_{e,R}} \tag{16}$$

The Rosseland approximation is valid when the medium absorbs and scatters isotropically (here we recognize that it is a strong assumption but it permits to get an acceptable estimation of radiative transfer). Using this assumption, $\sigma_{e,R}$ can be written as [eq. (17)]

$$\frac{1}{\sigma_{e,R}} = \int_0^\infty \frac{1}{\sigma_e\lambda}\cdot f_R(\lambda,T)d\lambda \tag{17}$$

where $f_R(\lambda,T)$ is the Rosseland distribution defined as

$$f_R(\lambda,T) = \frac{15}{4\pi^4}\left[\frac{hc}{\lambda k_B T}\right]^3\frac{1}{\lambda}\frac{\exp(hc/\lambda k_B T)}{[\exp(hc/\lambda k_B T)-1]^2}$$

where c is the velocity of light in vacuum, h is the Planck's constant and k_B is the Boltzmann's constant.

For the intermediate temperatures, most thermal energy radiates in the spectral range between 2 and 15 μm approximately. It can be evaluated using a Fourier Transform InfraRed (FTIR) spectrometer (Nicolet Impact 400D in this work) measuring the transmittance, $T_{n\lambda}$, spectrum of the sample. The spectral extinction coefficients for thin samples can be obtained using the Beer's law [eq. (18)][18]

$$T_{n\lambda} = \exp\left(-\int_0^L \sigma_{e\lambda}dx\right) \tag{18}$$

where $T_{n\lambda}$ is the spectral transmittance and L is the thickness of the sample. If the sample is homogeneous (in our case it is a reasonable assumption) then $\sigma_{e\lambda}$ is independent of x and eq. (18) becomes eq. (19)

$$\sigma_{e\lambda} = -\ln(T_{n\lambda})/L \tag{19}$$

The Rosseland mean extinction coefficient, $\sigma_{e,R}$, can be then calculated using eq. (17) and k_r using eq. (16).

Carbtex NW was carefully cut off to make 1 mm thick samples and FTIR spectrum was acquired in the transmission mode [Fig. 6(a)]. Transmittance as

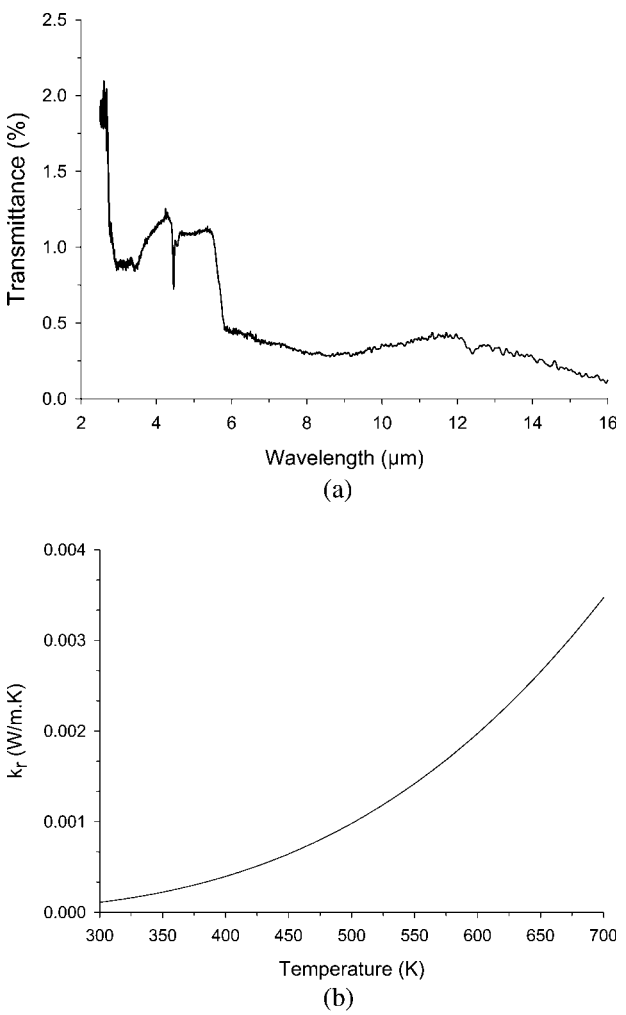

Figure 6 FTIR spectrum of 1 mm thick sample of Carbtex NW (a) and the resulting calculation of k_r as a function of temperature (b).

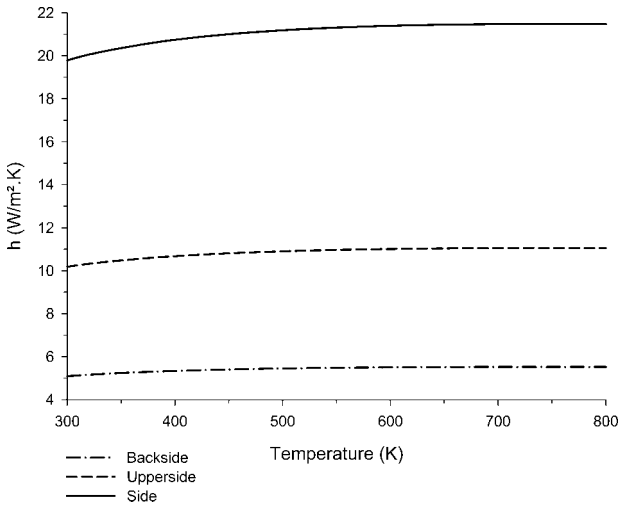

Figure 7 Calculated convection coefficients as a function of temperature on the backside, the upper side and the sides of the setup aluminum + Carbtex.

function of the wavelength is relatively low and the resulting calculated k_r remains also low increasing as a function of the temperature [Fig. 6(b)].

Convection coefficient

The convection coefficient was calculated using the simple empirical correlations for the average Nusselt number, Nu, in natural convection as [eq. (20)][20]

$$Nu = \frac{h\delta}{k} = C\,Ra^m \tag{20}$$

where C is a constant coefficient, m a constant exponent, δ is a characteristic length of the considered geometry, h is the convection coefficient, k the heat conductivity (here the air) and Ra is the Rayleigh number which is the product of the Grashof and Prandtl numbers [eq. (21)][20]

$$Ra = Gr\,Pr = \frac{g\beta(T_{\text{surf}} - T_\infty)\delta^3}{\nu\,\alpha} \tag{21}$$

where g is the gravitational acceleration, β is the coefficient of volume expansion (calculated as $\beta = 1/T$ assuming that the air is an ideal gas), ν is the kinematic viscosity of the fluid (air), T_{surf} is the temperature of the surface, T_∞ is the temperature of the air sufficiently far from the surface (here 300 K) and α is the thermal diffusivity.

The values of the constants C and m depend on the geometry of the surface and on the flow regime. According to the design of our test, it is reasonable to assume a laminar flow and so, m was set to 0.25.[20] The constant C is 0.54 for a horizontal plate (hot surface) and was set in our model for the upper side (NW). For the side (NW + aluminum plate), C was set to 0.59 (case of vertical plate) and for the backside (case of a lower surface of hot plate), C was set to 0.27.[20] All calculations for h were done assuming that air was at the film temperature ($T = 0.5 \times [T_{\text{surf}} + T_\infty]$). As it can be observed on the Figure 7, the convection coefficients are almost constant as a function of temperature and average values will be used in the modeling (see Table I).

TABLE I
Parameters and their Values Used in the Computation

Parameter	Value[a]
Density, ρ	$\rho_{\text{Carb}} = 1200$ kg/m^3
Heat capacity, c_p	$\rho_{\text{air}} = p.28.8.10^{-3}/(8.314.T)$ kg/m^3
	$c_{p\_\text{Carb}} = 3000$ J/kg K
	$c_{p\_\text{air}} = 1100$ J/kg K
	$c_{p\_\text{alu}} = 1296.6 - 4714/\ln T$ J/kg K
Heat conductivity, k	$k_{\text{Carb}} = 1$ W/m K
	$k_{\text{air}} = 10^{(-3.723+0.865.\log T)}$ W/m K
	$k_r = \exp[17.74 - (153.31/\ln T)]$ W/m K
	$k_{\text{alu}} = [2.4 + 0.084.\text{T}^{0.5}]^2$ W/m K
Volume ratio fiber/air, V_r	0.33
Randomly oriented fibers, Z	0.66
Surface temperature of the heat radiator	1000 K
Porosity, φ	0.75
Emissivity, ε	$\varepsilon_{\text{backside}} = 0.92$
	$\varepsilon_{\text{Carb}} = 0.95$
Stefan–Boltzmann constant, σ	$5.67.10^{-8}$ W/ṁ K^4
Convection coefficient, h	$h_{\text{side}} = 21$ W/ṁ K
	$h_{\text{upperside}} = 11$ W/ṁ K
	$h_{\text{backside}} = 5$ W/ṁ K

[a] Subscripts Carb is related to Carbtex NW, alu is related to aluminum and air is related to air.

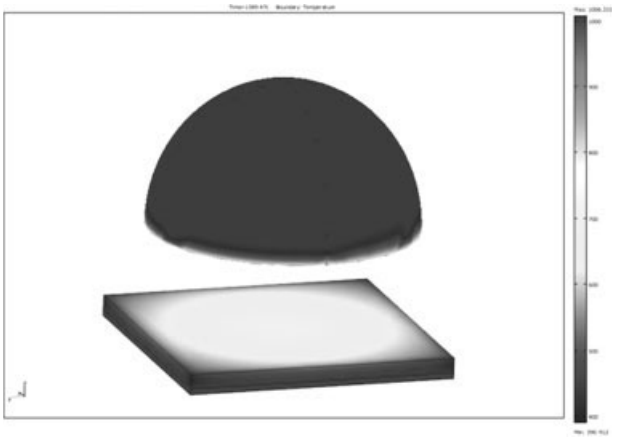

Figure 8 Boundary temperature on the assembly NW and aluminum plate during the heat radiator test (t = 1400 s).

Finite element calculation

The next step of our work is to solve the equations presented in the previous section on a 3 dimensional geometry. The required parameters are intrinsic properties of the material (PAN in NW) and of the fluid (air). They may depend on temperature as shown in Table I. Here we assume that the emissivity of Carbtex is constant equaling 0.95.

The equations presented in the previous section have been implemented in the commercial package Comsol Multiphysics and have been solved numerically on a three dimensional geometry using finite-difference approximations with the prescribed boundaries and with the values of Table I. The problem to be solved is highly nonlinear and the time-dependent solver was chosen. The algorithm of the time-dependent solver is based on the FEM discretization of the time-dependent PDE problem:

$$0 = L(U, \dot{U}, \ddot{U}, t) - N(U, t)^T \Lambda$$
$$0 = M(U, t)$$

where U is the solution vector, Λ is the Lagrange multiplier vector, L is the equation residual vector, N is the constraint Jacobian matrix, and M is the constraint residual vector. It is often referred to as the method of lines. Before solving this system, the algorithm eliminates the Lagrange multipliers Λ. If the constraints $0 = M$ are linear and time independent the algorithm also eliminates them from the system. Otherwise it keeps the constraints, leading to a differential-algebraic system. The solver is an implicit time-stepping scheme, which implies that it must solve a possibly nonlinear system of equations at each time step. It solves the nonlinear system using Newton iteration, and it then solves the resulting systems with an arbitrary linear system solver. The details of the whole calculation are described in.[19]

In the time-dependent solver, the time stepping was specified to be 1 s over the range 0–1400 s. It is also essential for accuracy to set absolute and relative tolerance parameters for the time-dependent solver. The absolute and relative tolerances, set at 0.001 and 0.01, respectively, control the error in each integration step. More precisely, let U be the solution vector corresponding to the solution at a certain time step, and let E be the solver's estimate of the (local) error in U committed during this time step. The step is accepted if

$$\left[\frac{1}{N}\sum_i \left(\frac{|E_i|}{A_i + R|U_i|}\right)^2\right]^{1/2} < 1$$

where A_i is the absolute tolerance for DOF i, R is the relative tolerance, and N is the number of degrees of freedom.

Figure 8 shows temperature gradient on the boundaries of the assembly aluminum plate and NW. As expected temperature is the highest in the center of NW (about 700 K at 1400 s) and the temperature on the sides remains relatively low because of heat losses (about 530 K at 1400 s).

Figure 9 compares simulated and measured temperatures as a function of time on the backside of the aluminum plate (temperature on the center of the plate). The simulated curve exhibits an excellent fit regard to the experimental one. Six other temperature profiles were recorded at different locations (4 points at 1.5 mm from the center on the two diagonals and 2 points at 1 mm from the sides) on the backside of the aluminum plate and they were com-

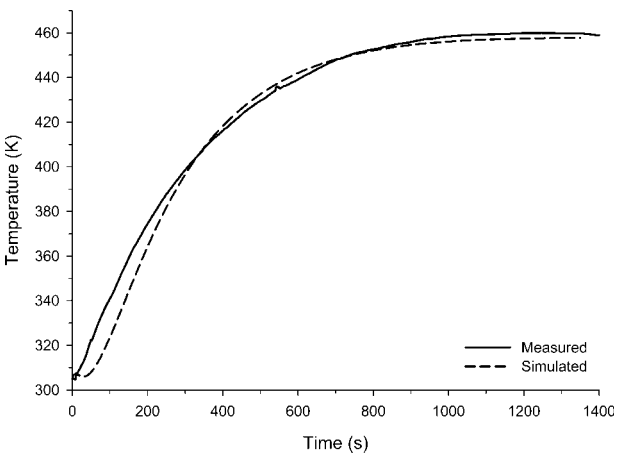

Figure 9 Measured and simulated temperatures as a function of time on the backside of aluminum plate (temperature on the center of the plate).

pared with the simulated curves. The predictions are similar as that presented on Figure 9. The difference between predicted and measured temperatures has an average value of 3.8 K and a standard deviation of 4.5. Considering that the numerical predictions have certain uncertainty associated to the thermophysical properties of Carbtex NW in addition to the experimental measures (estimated maximum uncertainties in the temperature measurement and location error are ±0.5 K and ±0.1 mm), the overall agreement is quite satisfying. It then validates our macroscopic approach of the model and it suggests that our model permits a good prediction of the behavior of NW as heat barrier.

The velocity fields of air in the Carbtex NW are plotted as a function of time (Fig. 10). The simulated values are very small suggesting that convection phenomenon may be ignored in the modeling of heat transfer in fibrous materials.

Temperature profiles as a function of time and of depth are also examined using the data of the computation (Fig. 11). The temperature difference between the surface and the backside of aluminum plate is of 230 K which demonstrates the efficiency NW as heat barrier. It is noteworthy that temperature of aluminum is the same at the interface aluminum/NW and on its backside. It makes sense because the thermal diffusivity of aluminum is high and the thermal response of the plate is therefore rapid.

Numerical simulation

Experimental results have validated our model and numerical simulations have been performed varying different parameters to examine the influence of the properties, of the structure and of the design on the performance of NW. Numerous high performance

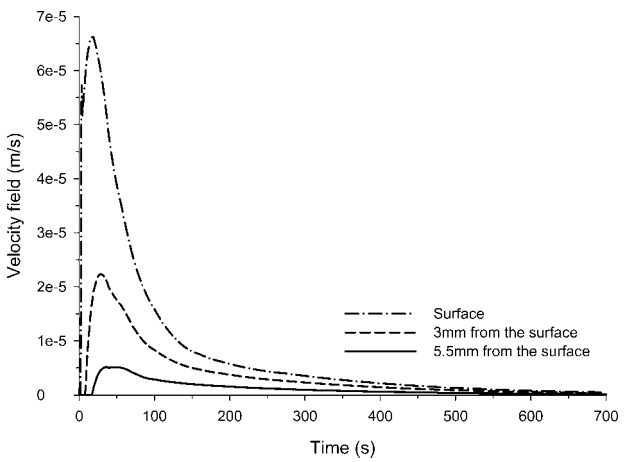

Figure 10 Velocity field as a function of time in the fibrous Carbtex NW at different depth and in the center.

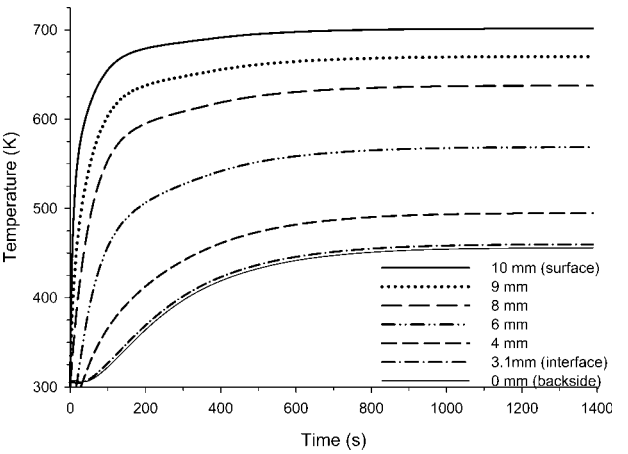

Figure 11 Simulated temperature profile as a function of time in the center of the material (0 is taken on the backside of the plate (3 mm thick) and the surface correspond to a total thickness of 10 mm (7 mm thick NW layer).

fibers (aramid fibers, polyimide fibers, carbon fibers, metallic fibers, ceramic fibers . . .) are available on the market exhibiting a broad range of properties (e.g., heat conductivity).[11] Depending on the polymer used and the structure of the fiber, heat conductivity may strongly vary. Our interest is to perform calculation with different values of k (lying from 0.5 to 10 W/m K and keeping all other parameters constant) and to simulate the temperature as a function of time on the backside of the aluminum plate as we did in our experiments (Fig. 12). As we can expect the lower the heat conductivity, the lower the temperature is. The temperature difference is of about 100 K at 1400 s for NW exhibiting k of 0.5 and 10 W/m K. This difference is of interest to get better insulation and so the fiber should be carefully chosen according to the required specification.

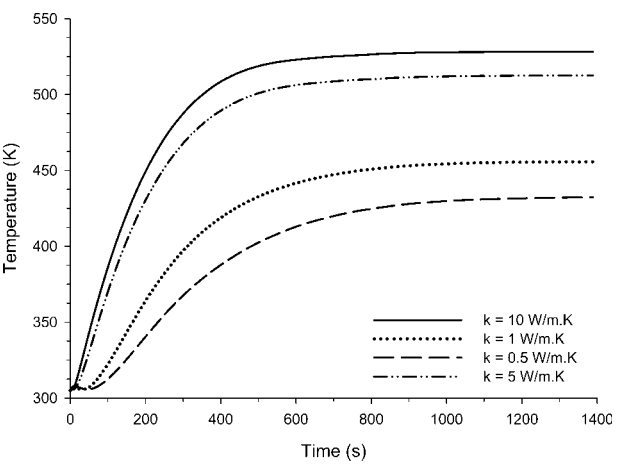

Figure 12 Simulated temperatures as a function of time on the backside of aluminum plate (temperature on the center of the plate) varying the heat conductivity, k, in the calculations.

Air is embedded in the NW structure and a porous medium is created. We may then expect increasing the performance of the heat barrier playing with the NW structure to make NW with large porosity. It is observed calculating the curves of temperature versus time varying the porosity from 0.25 to 0.9, a relatively large temperature difference of 90 K (at 1400 s) associated with a relatively slow heating rate (Fig. 13). Note that at $\varphi = 0.25$, the efficiency of NW layer is relatively poor in terms of temperature reached at the equilibrium (510 K versus 540 K) even if the heating is strongly reduced. As the thermal conductivity of fibers, the porosity of NW is therefore crucial to get the best efficiency. Keeping in mind that the surface temperature of NW in those conditions is of about 700 K, the temperature difference between the backside and the surface can reach up to 300 K ($\varphi = 0.9$).

The thickness of the protective layer acting as heat barrier is also a parameter of interest to optimize the performance. Temperatures as a function of time have been simulated on the backside of the aluminum plate varying the thickness (from 3 to 9 mm) of the NW put on the plate (Fig. 14). It is observed that the thicker the layer of NW, the better is the efficiency. It is noteworthy that the highest calculated surface temperature (9 mm thick layer of NW) reaches 720 K at the equilibrium but it remains below the temperature of degradation of Carbtex NW. Thermogravimetric curve (not shown) reveals that Carbtex NW exhibits its main step of degradation in thermo-oxidative conditions (air flow) at 730 K. From 3 mm thick, the layer start to be efficient (40 K temperature difference without and with NW layer) but from 5 mm the efficiency jumps from 40 to 80 K in terms of temperature difference with and without NW layer and finally it reaches 105 K with 9 mm NW layer. From these results, we may suggest that 5 mm thick of NW layer (our experimental measurements were done with a 7 mm thick Carbtex NW) should be the right compromise to get an acceptable efficiency of the heat barrier and to avoid potential further degradation of Carbtex.

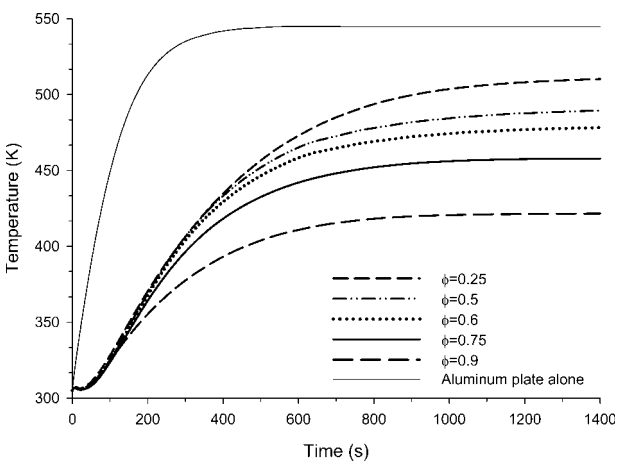

Figure 13 Simulated temperatures as a function of time on the backside of aluminum plate (temperature on the center of the plate) varying the porosity, φ, in the calculations.

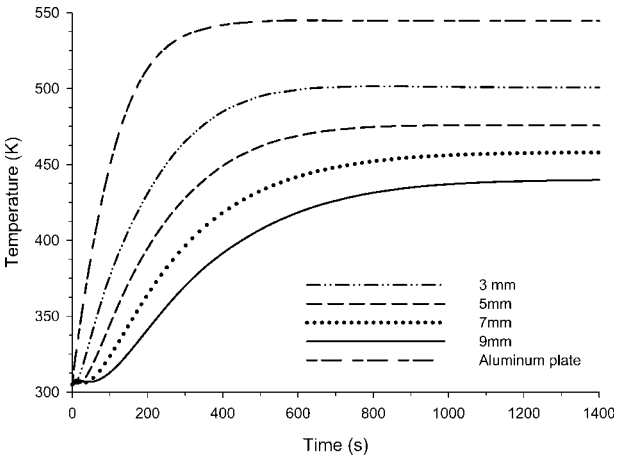

Figure 14 Simulated temperatures as a function of time on the backside of aluminum plate (temperature on the center of the plate) varying the thickness of NW on the plate.

CONCLUSIONS

A macroscopic model has been developed to simulate heat transfer in NW (considered as a porous medium) used as a protective heat barrier on aluminum plate. The model has been validated comparing experimental results obtained from a heat radiator test made in our laboratory and modeled results. The efficiency of NW layer has been simulated varying different parameters characteristic of the NW (porosity and heat conductivity) and of the design (thickness of the layer). It is revealed to get good efficiency of the NW heat barrier that heat conductivity of the fibers is crucial to get superior performance as well as high porosity (higher than 0.5) associated with a reasonable thickness of NW (5–7 mm).

The authors are indebted to Miss Maude Jimenez from our group for participating in this work and for helpful discussion. Miss Clémence Rawas and Mr. François-Xavier Delatte from Duflot Industries are gratefully acknowledged for helpful collaboration and discussion.

References

1. Aizenshtein, E. M. Fibre Chem 2005, 37, 307.
2. Michielsen, S.; Pourdeyhimi, B.; Desai, P. J Appl Sci 2006, 99, 2489.
3. Gardner, E.; Grady, P. L.; Mohammed, M. J Eng Ind 1984, 102, 214.

4. Obendorf, S. K.; Smith, J. P. Textile Res J 1986, 56, 691.
5. Farnworth, B. Textile Res J 1987, 57, 717.
6. Lee, S. C.; Cunnington, G. R. J Thermophys Heat Transfer 2000, 14, 4.
7. Savel'eva, E. K.; Dedov, A. V.; Bokova, E. S.; Andrianova, G. P. Fibre Chem 2005, 37, 202.
8. Asllanaj, F.; Jeandel, G.; Roche, J. R.; Lacroix, D. Int J Therm Sci 2004, 43, 939.
9. Kamdem Tagne, H. T.; Doermann Baillis, D. J Heat Transfer 2005, 127, 1115.
10. Bai, D.; Fan, X. J. J Quant Spectrosc Radiat Transfer 2007, 104, 326.
11. Bourbigot, S.; Flambard, X. Fire Mater 2002, 26, 155.
12. Jimenez, M.; Duquesne, S.; Bourbigot, S. Ind Eng Chem Res 2006, 45, 7475.
13. Bourbigot, S.; Le Bras, M.; Duquesne, S.; Rochery, M. Macromol Mater Eng 2004, 289, 499.
14. Incropera, F.; De Witt, D. Fundamentals of Heat and Mass Transfer, 4th ed.; Wiley: New York, 1996.
15. Verschoor, J. D.; Greebler, P.; Manville, N. J. J Heat Transfer 1952, 74, 961.
16. Fricke, J.; Stark, C. Int J Heat Mass Transfer 1993, 36, 617.
17. Boulet, P.; Jeandel, G.; Morlot, G. Int J Heat Mass transfer 1993, 36, 4287.
18. Siegel, R.; Howell, J. R. Thermal Radiation Heat Transfer; Taylor & Francis: London, 1992.
19. Brown, P. N.; Hindmarsh, A.C.; Petzold, L. R. SIAM J Sci Comput 1994, 15, 1467.
20. Bejan, A. Heat Transfer; Wiley: New-York, 1993.